scientific reports

Check for updates

OPEN

Characterising the anxiogenic network from functional connectivity analysis of the CO_2 challenge model

Daniel Graham[1,2,3]✉, Santra Mathew[1], Jonathan Marsden[1], Alastair D. Smith[1], Gary Smerdon[2] & Stephen D. Hall[1]

The CO_2 challenge model (CCM) is a gas inhalation paradigm that provides precisely controlled anxiety induction in experimental settings. Despite its potential as an experimental model of anxiety, our understanding of the neural effects of the CCM is incomplete. This study employs resting-state functional magnetic resonance imaging (rs-fMRI) to explore functional connectivity (FC) changes underlying the CCM. Following a preliminary CO_2 tolerance assessment, participants completed an MRI session that included three rs-fMRI scans: during inhalation of control air (pre and post), and during a 6% CCM exposure. Here, we confirm that 6% CCM is a tolerable anxiogenic model in the MRI setting. We demonstrate that a transient CCM-induced increase in subjective anxiety is associated with an increase in FC within limbic and anxiety-related regions, with the insula emerging as a central node in this altered connectivity pattern. Further analysis revealed a significant correlation between the levels of subjective anxiety and enhanced FC between the brainstem and medial frontal cortex, highlighting the dynamic role of the brainstem in response to CO_2-induced anxiety. These findings underscore the value of combining CCM and rs-fMRI to characterise the neural mechanisms of anxiety, with important implications for evaluating potential therapeutic interventions.

Anxiety disorders affect 3–4% of the global population and pose a significant public health challenge, impacting quality of life, social relationships, and occupational productivity[1,2]. These disorders are characterised by high comorbidity with other mental illnesses and often manifest early in life[3]. However, anxiety is a functionally ubiquitous psychological experience, exhibiting a wide spectrum of cognitive, emotional, and physiological symptoms that vary substantially between individuals. Such variability underscores the complexity of anxiety, which is influenced by diverse factors including neurochemical, metabolic, neuroanatomical, genetic, respiratory, and cognitive components; each empirically validated[4]. Yet, despite the substantial human and socioeconomic implications, the underlying mechanisms of anxiety remain inadequately understood, highlighting the critical need for further research in this domain[5].

Human research on anxiety primarily focuses on two areas: (i) identifying differences between patients with anxiety disorders and healthy controls, and (ii) investigating the dynamics of experimentally induced anxiety compared to a baseline condition. Such studies have advanced our understanding of anxiety and highlight the involvement of several brain regions in pathological anxiety, including (but not limited to) the amygdala, hippocampus, prefrontal cortex, and insula[6–9]. However, the broad spectrum of anxiety disorder subtypes, and the high prevalence of psychiatric comorbidity, underscore a complex heterogeneity. For example, social anxiety is accompanied by abnormal processing in the cingulate gyrus, illustrating the specificity of neural correlates within subtypes of anxiety[9]. These factors present obstacles to establishing underlying mechanisms and causality.

In contrast, experimental models that employ active paradigms to induce anxiety in healthy subjects, such as exposure to fearful faces or unpredictable threats, offer the advantage of producing more consistent and controlled anxiety responses across participants. This homogeneity provides a clearer understanding of anxiety mechanisms compared to studies of pathological anxiety, where the variability in individual symptoms and comorbid conditions can complicate the interpretation of results. However, while a recent meta-analysis of neuroimaging research validates the involvement of key brain regions linked to pathological anxiety, it highlighted inconsistent neural networks across experiments[10]. The variability in individual responses to anxiety-

[1]University of Plymouth, Plymouth, UK. [2]DDRC Healthcare, Plymouth, UK. [3]Brain Research & Imaging Centre, University of Plymouth, Plymouth Science Park, Research Way, Plymouth PL6 8BU, UK. ✉email: daniel.graham@students.plymouth.ac.uk

inducing stimuli, combined with the active engagement required in these task-based models, creates challenges in characterizing anxiety's effects. Limiting the applicability of these models when studying how anxiety impacts cognitive and behavioural functions, as individual differences can obscure the underlying neural mechanisms being investigated.

Bridging this gap, the CO_2 challenge model (CCM) presents a robust experimental approach to eliciting transient anxiety by administering elevated levels of inhaled CO_2[11]. The CCM typically applies 7.5% CO_2 to induce central and peripheral chemoreceptor-mediated changes in the central nervous system, autonomic nervous system, and vascular tone, reliably inducing a state of heightened anxiety that is observable across species[12]. The passive nature of the CCM enables researchers to study the influence of anxiety on a range of cognitive and behavioural functions in both healthy individuals and those with medical conditions[13,14]. Notably, the model's anxiety effects can be mitigated by central, but not peripheral, anxiolytic medications, highlighting its relevance as a proxy for studying generalised anxiety disorder (GAD)[15].

A handful of studies have looked at the effects of the CCM on neural activity. Goosens et al. (2014) used a boxcar design to compare the brainstem response to alternated 2-minute inhalation of 100% O_2 and 7% CO_2, in panic-disorder patients and low-sensitivity controls. Their results demonstrated a positive relationship between the amplitude of the participant anxiety response and activity in brainstem nuclei and insula[16]. A more recent study used fMRI to determine network connectivity in response to an emotional-faces task and showed a significant correlation between prefrontal cortex and amygdala activation and anxiety response in a subsequent 'offline' CCM experiment[17]. However, despite the potential of the CCM as a model of anxiety in healthy controls, neither the brain-wide network underlying its effects, nor the associated changes in functional connectivity, have yet been modelled.

In the present study, we address this knowledge gap by combining the CCM with rs-fMRI, alongside subjective measures of anxiety. A two-stage approach was adopted, in which an initial unbiased exploratory whole-brain analysis was used to confirm the network changes in response to CCM compared to control air. This provided the localisation of an 'anxiogenic network' (AGN), which was then used to guide a theory-driven analysis of functional connectivity change associated with anxiety. This AGN was then further investigated by examining changes in subjective levels of anxiety, and the dynamic nature of the AGN. We hypothesised that structures of known importance in anxiety, such as the limbic system, brainstem, and frontal areas, would show modulation in the CCM. We also predicted that changes in FC would positively correlate with state-anxiety scores.

Methods

Participants

Thirty-seven healthy participants (25 female, 12 males) aged 19 to 54 years ($M = 24.0$, $SD = 7.8$) were recruited to the study. Exclusion criteria included a current diagnosis of neurological or psychiatric disorders, current use of medications known to affect cortical excitability, pregnancy, use of psychoactive drugs, contraindications to MRI, and a history of respiratory disorders. Ethical approval was obtained for the study from the University Research Ethics Committee and informed consent was obtained from all participants following briefing of the experimental procedures. The methods were performed in accordance with the relevant guidelines and regulations. All experiments were conducted at the Brain Research & Imaging Centre (BRIC) at the University of Plymouth.

Pilot studies

Pilot studies with 5 volunteers tested the feasibility of CCM in the MRI environment as well as to determine the optimal CO_2 level. Our initial trials using the commonly applied 7.5% CO_2 model was found to be intolerable for several participants in the MRI environment. We subsequently used a 5% CO_2 model, which was tolerable, but participants did not reliably report an increase in anxiety. Consequently, we applied a 6% CO_2 model, which was found to be both tolerable and anxiogenic. Therefore the 6% CCM was adopted for the full study, to optimise anxiety induction, while minimising participant discomfort, movement, and attrition.

Screening phase

Prior to the MRI experimental phase, participants underwent preliminary screening to assess suitability, based on tolerance of the CCM. A 3-minute 6% CO_2 exposure was completed in a non-MRI lab environment, during which participants' heart rate and blood-oxygen saturation were continuously monitored to ensure safety and comfort. This screening phase optimised compliance in the MRI experiment, by identifying non-tolerance to the CCM and familiarising participants with the breathing apparatus.

Anxiety measures

Anxiety was assessed using the State-Trait Anxiety Inventory (STAI)[18]. The trait scale (STAI-t) was completed once at the start of the study, to determine potential interaction with subsequent state responses. The state scale (STAI-s) was completed before entering the MRI scanner room and again immediately following exit from the scanner room (approximately 10 min after the end of the CCM in the scanner). In addition, a repeated assessment of anxiety was made at intervals throughout the rs-fMRI experiment, using a Visual Analog Scale of anxiety (VAS-a). The VAS-a was used to capture participant ratings of anxiety within the current experimental block, on a scale from 1 ("not at all anxious") to 10 ("extremely anxious").

CCM protocol

The MRI study used two gas mixtures, delivered via a Douglas bag with a non-rebreathing valve: (1) control air (0.04% CO_2) and (2) the CCM mixture (6% CO_2, 21% O_2, 73% N_2). Participants underwent three rs-fMRI scans: during baseline air (pre-air), CCM exposure (CCM), and air after CCM exposure (post-air). The pre-air

and post-air scan conditions used an identical respirator arrangement to the CCM condition, to account for non-CCM effects on FC. Therefore, the pre-air condition provided a true baseline, while CCM and post-air scans allowed for the identification of connectivity changes induced by the anxiogenic stimulus and recovery to baseline respectively. This ensured that observed CCM effects were transient and due to altered gas-mixture. See Fig. 1 for the experimental timeline.

MRI protocol

Participants were positioned comfortably supine in a 3-Tesla MRI scanner (Siemens Prisma, Erlangen, Germany) with a 32-channel head coil. Prior to the rs-fMRI experiment, a high-resolution anatomical sequence was acquired for coregistration of all subsequent functional data (MPRAGE; TR = 2100 ms, TE = 2.26 ms, TI = 900 ms, flip angle = 8°, GRAPPA acceleration = 2, FOV = 256 × 256 mm^2, 176 slices and 1 mm^3 isotropic voxels). Resting-state fMRI data were captured in three separate scans, with the start of the middle scan coinciding with the start of the CO_2 inhalation. Each rs-fMRI scan consisted of a Centre for Magnetic Resonance Research (CMRR) multiband rs-fMRI EPI sequence (https://www.cmrr.umn.edu/multiband/) with interleaved slice acquisition (TR = 2000 ms, TE = 30 ms, TA = 7 min, flip angle = 74°, FOV = 256 × 256 mm^2, voxel size of 3.2 × 3.2 × 2.5 mm^3, and 30 slices per volume, 200 volumes). During scans, a pulse oximeter attached to one hand enabled continuous physiological monitoring, and a call bell enabled participants to signal discomfort if required. Before each rs-fMRI scan there was a short rest of ~ 1 min during which the VAS-a scores were recorded, and comfort was assessed. VAS-a was also measured immediately after the participants left the MRI.

Rs-fMRI analysis

One participant withdrew during the screening phase and another during the MRI phase (due to intolerance of the CO_2 inhalation). Thirty-five participants completed all phases of the experiment.

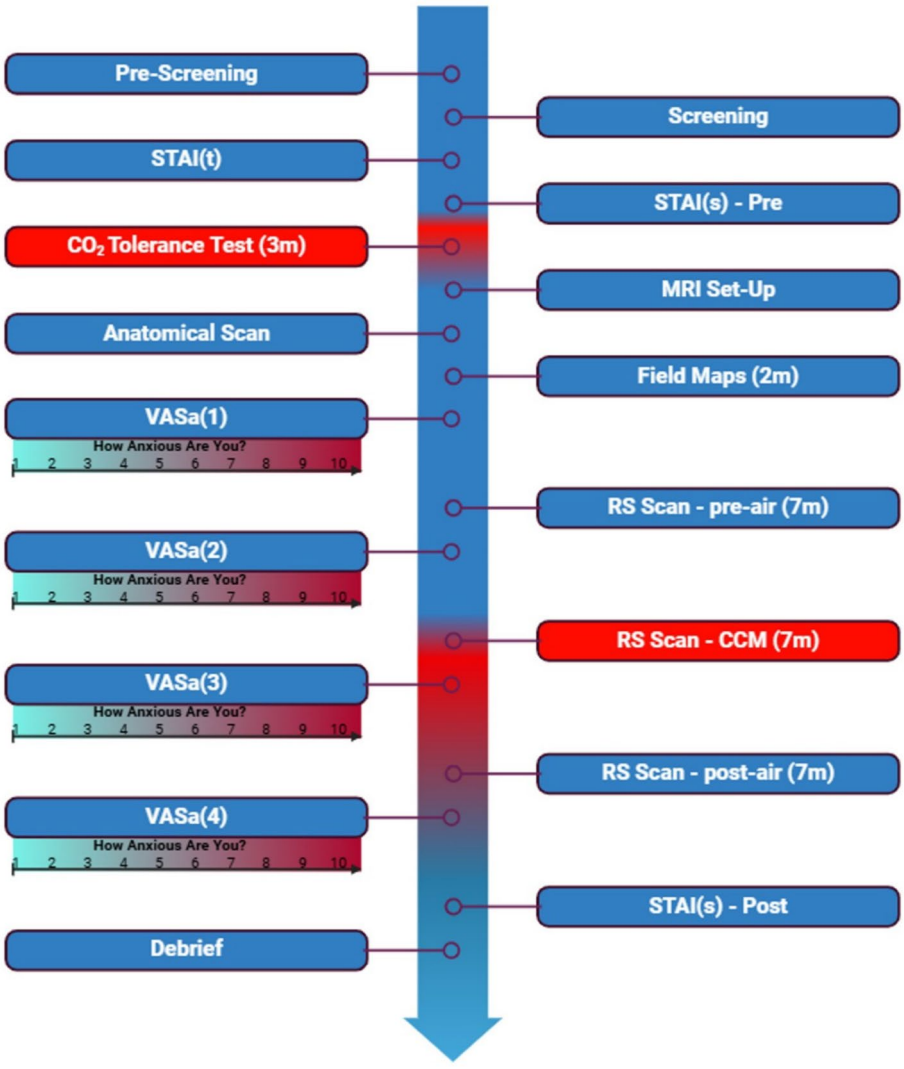

Fig. 1. Timeline of experimental procedure. Created in https://BioRender.com.

Pre-processing

Functional and anatomical data were processed using a flexible preprocessing pipeline[19]. This included: creation of voxel-displacement maps, susceptibility distortion correction using fieldmap realignment, slice timing correction, outlier detection, indirect segmentation, MNI-space normalization, and smoothing. Functional data were realigned and coregistered with the anatomical scan using the SPM realign & unwarp procedure[20], with distortion correction, a least squares approach, 6-parameter (rigid body) transformation, and resampled using b-spline interpolation[21] to simultaneously correct for motion, magnetic susceptibility geometric distortions, and their interaction. Temporal misalignment of functional data was corrected with the SPM slice-timing correction (STC) procedure[22,23] and potential outlier scans were identified using ART[24] as acquisitions with framewise displacement above 0.9 mm or global BOLD signal changes above 5 standard deviations[25,26]. All data were normalized into standard MNI space, segmented into grey matter, white matter, and CSF tissue classes, and resampled to 2 mm isotropic voxels following an indirect normalization procedure[26,27] using SPM unified segmentation and normalization algorithm[28,29] with the default IXI-549 tissue probability map template. Finally, functional data were smoothed using spatial convolution with a Gaussian kernel of 8 mm full-width half maximum (FWHM).

Denoising

Functional data were denoised using a standard denoising pipeline[30]. This included the regression of potential confounding effects characterized by: white matter time-series (5 CompCor noise components), CSF timeseries (5 CompCor noise components), motion parameters and first order derivatives (12 factors)[31], outlier scans (below 54 factors[25]), session and task effects and first order derivatives (6 factors), and linear trends (2 factors), within each functional run. BOLD timeseries were bandpass frequency filtered[32] (0.008 Hz and 0.09 Hz), and CompCor[33,34] white matter and CSF noise components were estimated by computing average BOLD signal and orthogonal principal components. The effective degrees of freedom in the BOLD signal post-denoising ranged from 146.3 to 167.3, with an average of 161.1 across participants[26].

First-level analysis

ROI-to-ROI connectivity (RRC) matrices were initially calculated for each pair of regions within 164 HPC-ICA networks[35] and Harvard-Oxford atlas ROIs[36]. Functional connectivity strength was quantified using Fisher-transformed bivariate correlation coefficients derived from a weighted general linear model (weighted-GLM[37]). The model accounted for the association between BOLD signal time series of each ROI pair, with individual scans weighted by task-specific boxcar signals convolved with SPM's canonical hemodynamic response function. This was then divided into two ROI-ROI analyses an exploratory and theory driven analysis. For the unbiased exploratory analysis, we selected 132 anatomical areas, including 91 cortical, 15 subcortical and 26 cerebellar parcellation areas according to Conn atlas apriori groups. For the subsequent theory-driven analysis, we defined the AGN based upon previously known anxiety-related regions, and our exploratory analysis. This AGN included the amygdalae, hippocampi, medial frontal cortex (MedFC), brainstem, thalamus, anterior cingulate cortex (ACC), and insulae. In whole-brain and AGN analysis, a connection-significance threshold of $p < 0.05$ (uncorrected) and cluster-significance threshold of $p < 0.05$ were applied with an FWE correction based on spatial extent.

Seed-based connectivity (SBC) maps were generated to characterize the connectivity patterns from specific seed regions (Harvard-Oxford atlas ROIs[36]) to all other brain voxels. Functional connectivity strength was similarly quantified using Fisher-transformed coefficients from a weighted-GLM[37], focusing on the association between seed area time series and each target voxel. Individual scans were weighted by task-specific boxcar signals, as in the ROI-to-ROI analysis.

Group-level analyses

Group-level analysis was performed by estimating a general linear model (GLM[38]) for each individual voxel. The first-level connectivity measures at these voxels were used as dependent variables, with one independent sample per subject and one measurement per task or experimental condition, if applicable, and group or other subject-level identifiers as independent variables. Voxel-level hypotheses were evaluated using multivariate parametric statistics with random-effects across subjects and sample covariance estimation across multiple measurements. Inferences were performed at the level of individual clusters (groups of contiguous voxels). Cluster-level inferences were based on parametric statistics from Gaussian Random Field theory[39,40]. Results were thresholded using a combination of a cluster-forming $p < 0.001$ voxel-level threshold, and a familywise corrected $p\text{-}FDR < 0.05$ cluster-size threshold[41].

Results

Anxiety measurements

Analysis of anxiety measures from the VAS-a, using one-way repeated measures ANOVA, demonstrated a significant effect ($F(3, 78) = 14.14$, $p < 0.001$) of CCM on subjective anxiety scores with no significant change between the baseline and control air conditions. Although participants reported higher VAS-a subjective anxiety during CCM exposure, a within-subject analysis of pre and post-CCM subjective STAI-s scores showed no significant change in state anxiety ($t(46.85) = 1.20$, $p = 0.23$), indicating that there was no residual post-experiment anxiety following the cessation of CCM. These results confirm a transient increase in anxiety induced by the CCM, but no residual post-experiment anxiety as can be seen in Fig. 2.

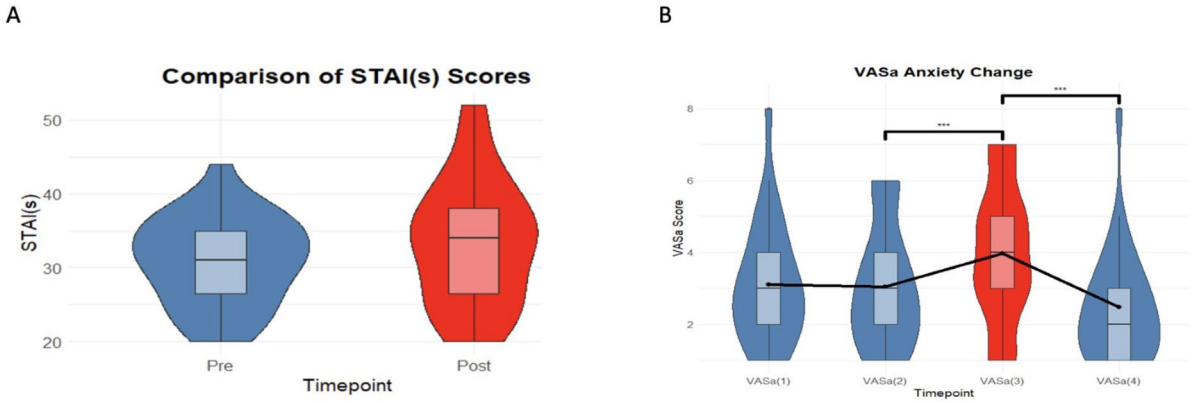

Fig. 2. Pre, peri and post CCM anxiety scores. (**A**) VAS-a scores indicating a significant increase (***$p < 0.001$) in anxiety rating during CCM exposure compared to pre-air. (**B**) Comparison of STAI-s anxiety scores before and after CCM exposure, showing no significant difference ($p = 0.23$) in residual anxiety.

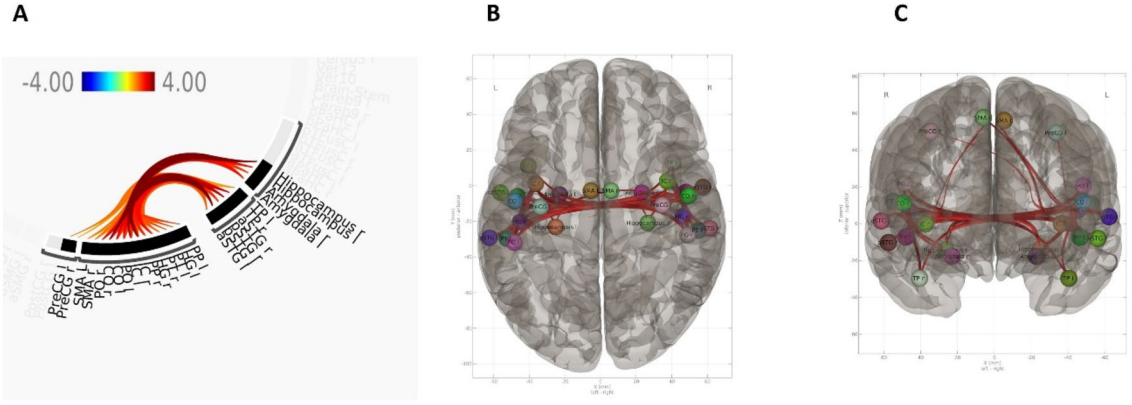

Fig. 3. Whole brain rs-fMRI. (**A**) Connectivity plot summarising clusters and regions in which increased FC was observed between CCM and pre-air condition. Showing one significant cluster increased FC, Mass = 1170.06, (p-$unc < 0.001$, p-$FDR = 0.041$, p-$FWE = 0.037$). No significant decreases in FC were found observed. (**B**,**C**) ROI-ROI connectivity results overlayed on superior (**B**), and anterior (**C**) brain template.

Whole brain rs-fMRI

Initial unbiased whole-brain analysis of 132 anatomical areas, explored connectivity changes in response to CCM compared to pre-air. This revealed increased FC primarily between the insula, hippocampus, amygdala, and central opercular cortex, being mostly localised over the central and limbic areas as can be seen in Fig. 3. No significant change in FC was observed between the CCM and post-air.

Anxiogenic network (AGN) rs-fMRI

To investigate CCM modulation of the AGN (amygdala, insula, thalamus, hippocampus, brainstem, ACC, and MedFC), we conducted a detailed analysis of FC within this predefined network in response to CCM anxiety compared to the pre-air scan. This identified a cluster of increased FC within the AGN during CCM exposure. In particular, strong changes in connectivity were observed bilaterally between the insula and critical AGN regions including the hippocampus, amygdala, brainstem, MedFC, and thalamus (Fig. 4). This underscores the central role of the insulae in the integration of sensory and emotional information, in the context of anxiety. Moreover, analyses revealed significant increases in FC between the ACC, thalamus, and brainstem, suggesting a sophisticated network coordinating cognitive control, emotional regulation, and autonomic responses during the induction of elevated anxiety. Involvement of the ACC suggests a central role in modulating cognitive processes in response to emotional stimuli, while the thalamus-brainstem axis likely reflects a fundamental increase in physiologically driven neural inputs. No significant change in FC was observed between the CCM and post-air scans.

Temporal profile of AGN dynamics

To determine the time course of the CCM-driven modulation of FC in the AGN, we employed a dynamic sliding window analysis. This approach utilised 180-second windows that advanced in 25-second steps. This provided a temporal representation of FC evolution in the AGN in response to CCM-induced anxiety. As can be seen

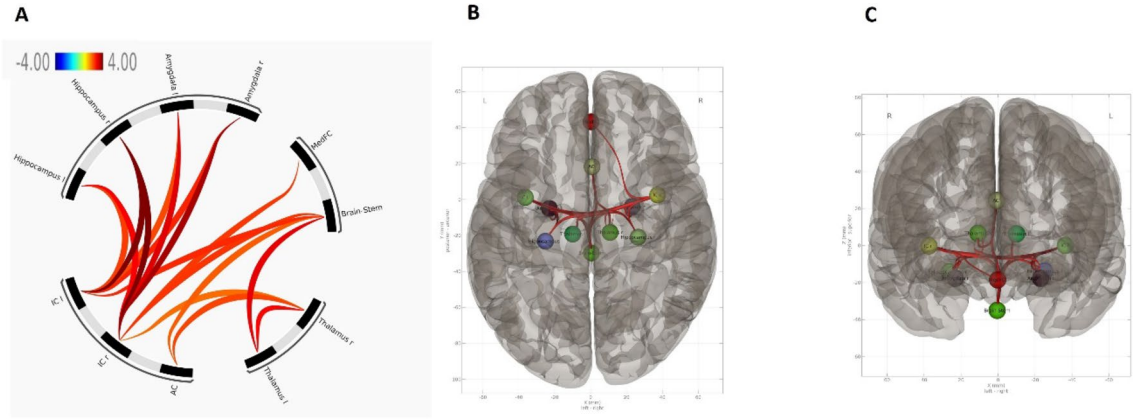

Fig. 4. AGN rs-fMRI. (**A**) Connectivity plot summarising clusters and regions in which increased FC was observed between CCM and pre-control air condition. Showing a significant cluster of increased FC, Mass = 296.20, (p-$unc < 0.001$, p-$FDR < 0.001$, p-$FWE < 0.001$). No significant decreases in FC were observed. (**B**,**C**) ROI-ROI connectivity results overlayed on superior (**B**), and anterior (**C**) brain template.

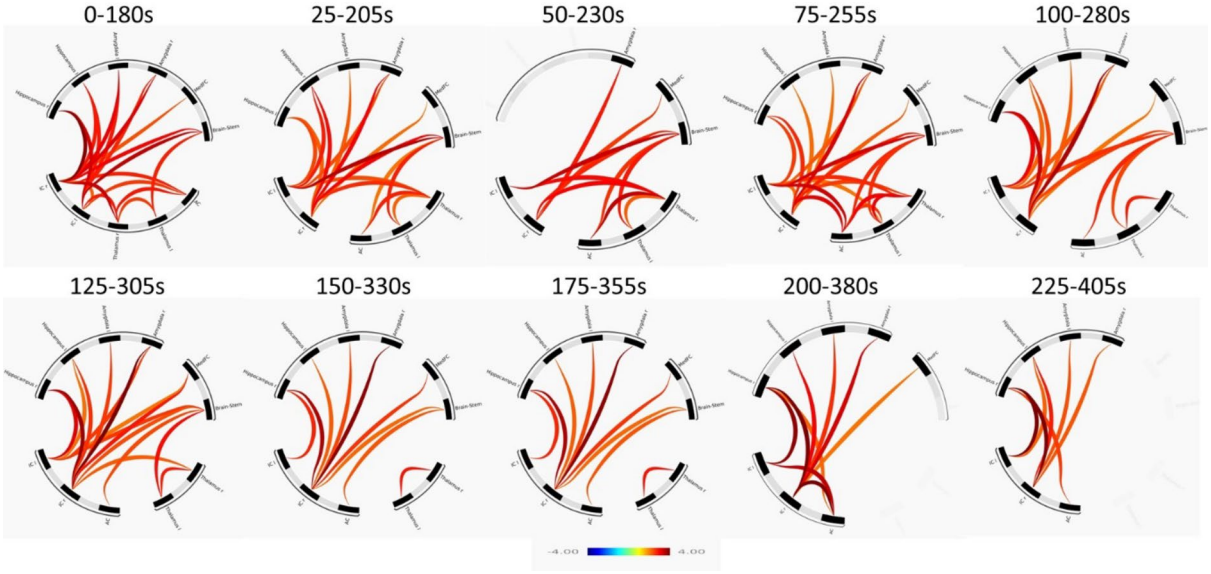

Fig. 5. AGN rs-fMRI connectivity cluster diagram. Connectivity plot summarising clusters and regions in which increased FC was observed over time. No significant decreases in FC were observed.

in Fig. 5 it was revealed that FC changed across the AGN in a manner that was consistent with the previous analysis (Fig. 3), with initial increases in FC in the brainstem and insula. Subsequently, towards the end of the CCM session, there was a notable reduction in the contribution of brainstem and thalamus to the AGN's overall connectivity.

Subjective anxiety and functional connectivity

Given individual variance and subjectivity in the experience of anxiety, we analysed the role of the AGN in subjective anxiety ratings during the CCM, using GLM analysis to correlate the strength of ROI-ROI connections and change in VAS-a ratings (pre-post CO_2 exposure). A significant increase in FC was found only between the brainstem and MedFC, occurring between the control air and CCM exposure ($F(1,24) = 10.27$, p-$unc = 0.004$, p-$FDR = 0.038$).

Seed-based analysis of the insula

Finally, based upon the apparent central function of the insula in the AGN (Figs. 3 and 4), we applied a seed-based using the insulae voxel coordinates. A voxel threshold $p < 0.001$ (p-uncorrected), and one-sided-sided cluster threshold $p < 0.05$ (cluster-size p-FDR corrected) confirmed widespread changes in connectivity including cerebellum, brainstem, amygdala thalamus, AC, and hippocampus as can be seen in Fig. 6. No significant change in FC was observed between the CCM and post-air.

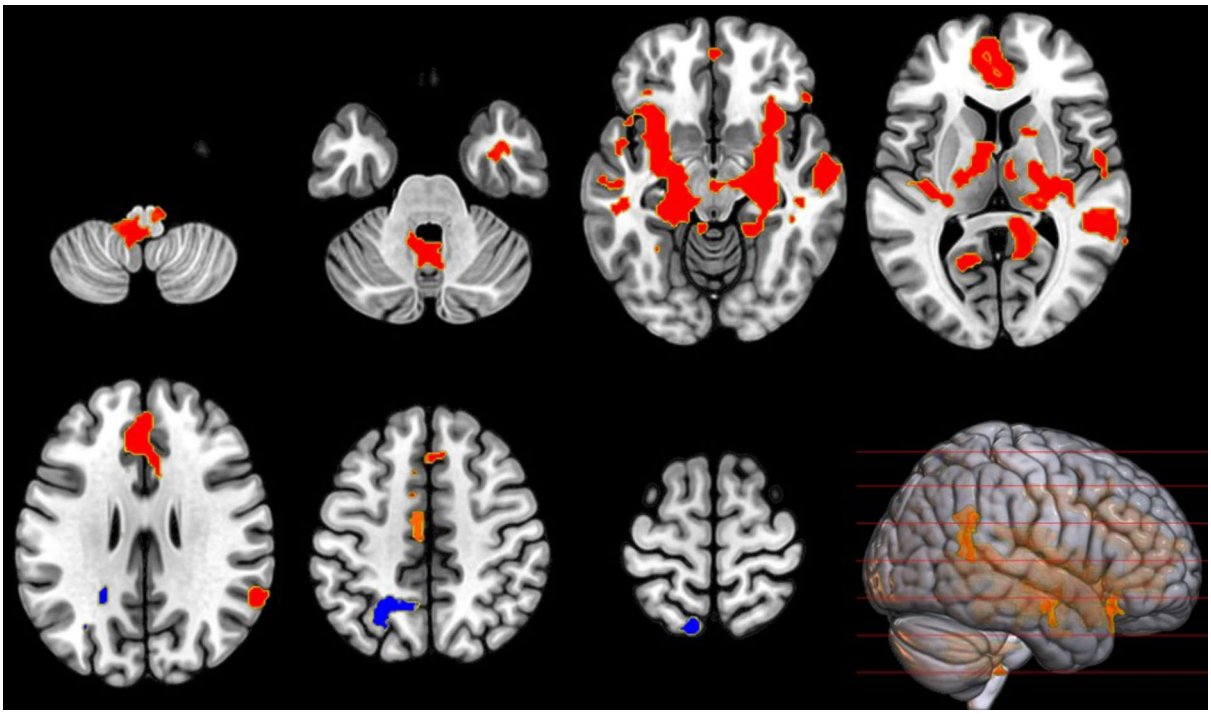

Fig. 6. Figure 6:Insula connectivity change during CCM. Illustrates the change in FC, with left and right insula as a seed, between baseline control air and CCM, showing a significant increase (red) in FC in three clusters (MNI coordinates [− 30, +16, − 08], [− 08, − 44, − 38], and [+50, − 36, +06]) all showing T(23) > 2.50, k ≥ 665. A single cluster showed a decrease (blue) in FC in the (MNI coordinates: [− 20, − 52, +42]) with T(23) > 2.50 and cluster size k ≥ 952.

Discussion

We demonstrate the successful integration of the CCM with rs-fMRI as a method of measuring changes in FC associated with the induction of anxiety. The application of an initial offline CCM screening protocol optimised compliance in an rs-fMRI experiment by confirming tolerance and familiarising participants with the protocol. Importantly, this study confirmed that the application of a 6% CO_2 model is both tolerable in the majority of participants (35 of 37) and elicits a reliable increase in anxiety, as reported with the VAS-a ($p < 0.001$).

Our initial pilot studies confirmed that tolerance of the typical 7.5% CO_2 model is reduced in the MRI environment. We propose that, particularly in participants that are naïve to MRI studies, this reflects an elevation in baseline state anxiety in this setting compared to a typical lab setting. While this is not surprising, given the comparative confinement and perceived serious nature of the scanner environment, it does raise important questions about the influence of MRI itself on anxiety. Specifically, while it is known that the MRI environment alters cognitive and perceptual performance in healthy controls[42] and patients[43], the present observations suggest that the contribution of anxiety may need to be more carefully considered.

Our findings demonstrate that while a robust increase in peri-experimental anxiety was achieved by the 6% CCM, there were no sustained post-experiment anxiety effects measurable with the STAI-s ($p = 0.23$). In fact, an absence of VAS-a difference between pre and post control air conditions suggests that anxiety effects subsided rapidly once CO_2 inspiration was discontinued. We therefore propose that the 6% CCM is an optimal method for studies investigating the neural effects of experimental anxiety using MRI. The passive nature of this intervention allows for quantification of AGN connectivity alongside testing with additional cognitive and behavioural paradigms. Moreover, the consistent and objective nature of the CCM and rs-fMRI allows studies to define FC-based differences in the AGN between healthy and patient populations. Importantly, quantification of AGN connectivity affords the opportunity to identify biomarker predictors of drug efficacy in treatment of anxiety disorders.

This study is the first to combine CCM and rs-fMRI to successfully identify an AGN based upon changes in functional connectivity. We demonstrate that changes in connectivity in the AGN were specific to the periods of elevated anxiety elicited by inhalation of elevated CO_2. Consistent with extensive literature, the AGN included brain regions of established importance in anxiety[6–8,10]. In particular, we observed robust changes in activity in the amygdalae, hippocampi, insulae, prefrontal cortex, thalamus, ACC, and brainstem. Importantly, we confirm that the AGN is characterised by increased connectivity between the insulae and a range of regions. Additionally, there were increases in FC with: the ACC, indicating heightened integration of emotional and cognitive processing[44]; the hippocampi, suggesting an increased involvement in memory processing[45]; and the amygdalae, which suggests an elevation in threat assessment and emotion regulation[46]. Moreover, an increase

in thalamic functional connectivity with both the insular cortex and ACC reflects its role in mediating wider cortical connectivity, which modulates the integration of sensory information[47].

Notably, an increase in connectivity between the brainstem, thalamus and insula cortices confirms previous observations of a central role in CCM-mediated autonomic responses. We propose that the consistency of this observation with previous research[16], employing a 2-minute boxcar paradigm suggests that the changes in brainstem activation are an early component of the network change. Our analysis of temporal dynamics confirmed early increases in functional connectivity between the brainstem and insula, which likely reflects a rapid brainstem chemoreceptor activation in response to a CO_2-mediated reduction in arterial and CSF pH. The related observation of increased insula activity is consistent with that reported by Goosens et al. (2014)[16], with a corresponding increase in FC with the brainstem. We suggest that this reflects communication and interaction with interoceptive processing, known to be a function of the insulae that is key in shaping the subjective experience of anxiety[48,49].

An increased FC between the insula-thalamus and thalamus-brainstem is consistent with a circuit that monitors and responds to dyspnoea. Accordingly, this thalamus-brainstem response is known to be impaired in congenital central hypoventilation syndrome patients with deficient ventilation response to hypercapnia[50]. In addition, the dynamic analysis of the AGN showed that these connections between the brainstem and thalamus were strongest at the beginning of the CCM but disappeared towards the end of the CCM while the limbic connections remained. Attenuation of this connectivity in later stages may reflect neural adaptation or habituation to the prolonged exposure to CO_2, reflecting a capacity to modulate the response to sustained anxiety-inducing stimuli. This nuanced temporal evolution of FC within the AGN underscores the complex and dynamic nature of the brain's response to induced anxiety, offering insights into the mechanisms through which the brain navigates, and potentially regulates, prolonged states of anxiety.

Notably, this study establishes an association between subjective anxiety levels and FC, particularly highlighting an increase in FC between the brainstem and the MedFC. This highlights the role of the MedFC in anxiety regulation, where it modulates emotional responses through its connections with key brain regions[51]. The MedFC is traditionally recognized for its capacity to exert top-down control over limbic structures like the amygdala, thus modulating fear and emotional responses. Specifically, the enhanced connectivity between the MedFC and the brainstem in response to heightened subjective anxiety may reflect a coordinated neural response aimed at managing autonomic and emotional aspects of anxiety[51]. This interplay likely represents an adaptive mechanism, engaging both the cognitive control centres of the MedFC and the autonomic regulatory functions of the brainstem, thereby providing a more comprehensive understanding of the neural substrates underlying anxiety states induced by the CO_2 challenge model. The present study expands upon previous studies by demonstrating extensive increases in FC between the insulae and ACC, known to serve as a hub that coordinates cognitive responses to emotional stimuli. Moreover, increased FC between insulae and limbic structures, including the amygdalae and hippocampi, confirm a parallel communication with structures that process memory, threat assessment and memory. We suggest that these modulations in connectivity represent changes in communication that follow increased activity in the insulae.

A potential limitation of this study lies in the uneven distribution of females and males providing an insufficient sample for sufficiently powered comparison. This may affect the generalisability of our findings, as gender differences in anxiety are well-documented, with research indicating that females generally report higher levels of anxiety and exhibit distinct neural responses compared to males[52,53]. Further research is required to determine demographic-related differences with larger and more diverse samples to understand how AGN FC changes are influenced by factors such as gender, age, and the presence of anxiety disorders. Notably, prior research by Goosens et al. (2014)[16] demonstrated that patients with panic disorders showed elevated FC between the brainstem and insula compared to controls. In contrast, experienced divers, likely accustomed to the physiological symptoms of CO_2-mediated anxiety, showed lower FC than controls in response to the CCM. These findings underscore the importance of accounting for individual differences in functional responses to anxiety and further highlight the need for stratified analyses to better understand these variations.

In conclusion, this study demonstrates the feasibility of integrating CCM and rs-fMRI to identify the AGN. The approach has considerable potential for understanding the contribution of anxiety, and its neural underpinnings, to cognitive and behavioural processes in health and disease. Moreover, it provides an opportunity to obtain the individual neural characterisation that underlies the nuanced response to stress and a set of additional biological variables for stratifying patient groups. Finally, the ability to define markers of anxiety network change provides viable mechanistic targets for both transient and longitudinal evaluation of treatment efficacy. These data act as a springboard for further development, and our future studies will focus on exploring the dose-dependency of CCM effects, examining long-term changes in functional connectivity, and investigating the potential therapeutic interventions that could modulate the identified anxiogenic networks.

Data availability

The datasets from the current study are available from the corresponding author on reasonable request.

Received: 26 June 2024; Accepted: 22 November 2024
Published online: 26 November 2024

References

1. Bandelow, B. & Michaelis, S. Epidemiology of anxiety disorders in the 21st century. *Dial. Clin. Neurosci.* **17**, 327–335 (2015).
2. Yang, X. et al. Global, regional and national burden of anxiety disorders from 1990 to 2019: results from the global burden of Disease Study 2019. *Epidemiol. Psychiatr. Sci.* **30**, e36 (2021).

3. Solmi, M. et al. Age at onset of mental disorders worldwide: large-scale meta-analysis of 192 epidemiological studies. *Mol. Psychiatry* **27**, 281–295 (2022).
4. Kyriakoulis, P. & Kyrios, M. Biological and cognitive theories explaining panic disorder: a narrative review. *Front. Psychiatry* **14**, 957515 (2023).
5. Woelbert, E., Lundell-Smith, K., White, R. & Kemmer, D. Accounting for mental health research funding: developing a quantitative baseline of global investments. *Lancet Psychiatry* **8**, 250–258 (2021).
6. Kenwood, M. M., Kalin, N. H. & Barbas, H. The prefrontal cortex, pathological anxiety, and anxiety disorders. *Neuropsychopharmacology* **47**, 260–275 (2022).
7. Xu, J. et al. Anxious brain networks: a coordinate-based activation likelihood estimation meta-analysis of resting-state functional connectivity studies in anxiety. *Neurosci. Biobehav. Rev.* **96**, 21–30 (2019).
8. Kolesar, T. A., Bilevicius, E., Wilson, A. D. & Kornelsen, J. Systematic review and meta-analyses of neural structural and functional differences in generalized anxiety disorder and healthy controls using magnetic resonance imaging. *Neuroimage Clin.* **24**, 102016 (2019).
9. Yu, X. et al. Cognitive neural mechanism of social anxiety disorder: a Meta-analysis based on fMRI studies. *Int. J. Environ. Res. Public Health* **18**, 5556 (2021).
10. Chavanne, A. V. & Robinson, O. J. The overlapping neurobiology of induced and pathological anxiety: a meta-analysis of functional neural activation. *AJP* **178**, 156–164 (2021).
11. Bailey, J. E., Dawson, G. R., Dourish, C. T. & Nutt, D. J. Validating the inhalation of 7.5% CO_2 in healthy volunteers as a human experimental medicine: a model of generalized anxiety disorder (GAD). *J. Psychopharmacol.* **25**, 1192–1198 (2011).
12. Leibold, N. et al. CO2 exposure as translational cross-species experimental model for panic. *Transl. Psychiatry* **6** (2016).
13. Savulich, G. et al. Acute anxiety and autonomic arousal induced by CO2 inhalation impairs prefrontal executive functions in healthy humans. *Transl. Psychiatry* **9**, 1–10 (2019).
14. Seddon, K. et al. Effects of 7.5% CO2 challenge in generalized anxiety disorder. *J. Psychopharmacol.* **25**, 43–51 (2011).
15. Diaper, A. et al. The effect of a clinically effective and non-effective dose of lorazepam on 7.5% CO2-induced anxiety. *Hum. Psychopharmacol. Clin. Exp.* **27**, 540–548 (2012).
16. Goossens, L. et al. Brainstem response to hypercapnia: a symptom provocation study into the pathophysiology of panic disorder. *J. Psychopharmacol.* **28**, 449–456 (2014).
17. Huneke, N. T. M., Broulidakis, M. J., Darekar, A., Baldwin, D. S. & Garner, M. Brain functional connectivity correlates of response in the 7.5% CO2 Inhalational Model of generalized anxiety disorder: a pilot study. *Int. J. Neuropsychopharmacol.* **23**, 268–273 (2020).
18. Manual for the State-Trait Anxiety. Inventory (Form Y1 – Y2) | Request PDF. https://www.researchgate.net/publication/235361542_Manual_for_the_State-Trait_Anxiety_Inventory_Form_Y1_-_Y2.
19. Nieto-Castanon, A. FMRI minimal preprocessing pipeline. In *Handbook of Functional Connectivity Magnetic Resonance Imaging Methods in CONN*, 3–16 (Hilbert, 2020).
20. Andersson, J. L., Hutton, C., Ashburner, J., Turner, R. & Friston, K. Modeling geometric deformations in EPI time series. *Neuroimage* **13**, 903–919 (2001).
21. Friston, K. J. et al. Spatial registration and normalization of images. *Hum. Brain. Mapp.* **3**, 165–189 (1995).
22. Henson, R. N. A., Buechel, C., Josephs, O. & Friston, K. J. The slice-timing problem in event-related fMRI. *NeuroImage* **9**, 125 (1999).
23. Sladky, R. et al. Slice-timing effects and their correction in functional MRI. *Neuroimage* **58**, 588–594 (2011).
24. Whitfield-Gabrieli, S., Nieto-Castanon, A. & Ghosh, S. Artifact detection tools (ART). **7**, 11 (2011).
25. Power, J. D. et al. Methods to detect, characterize, and remove motion artifact in resting state fMRI. *Neuroimage* **84**, 320–341 (2014).
26. Nieto-Castanon A. Preparing fMRI Data for Statistical Analysis.
27. Calhoun, V. D. et al. The impact of T1 versus EPI spatial normalization templates for fMRI data analyses. *Hum. Brain Mapp.* **38**, 5331–5342 (2017).
28. Ashburner, J. & Friston, K. J. Unified segmentation. *Neuroimage* **26**, 839–851 (2005).
29. Ashburner, J. A fast diffeomorphic image registration algorithm. *Neuroimage* **38**, 95–113 (2007).
30. Nieto-Castanon, A. FMRI denoising pipeline. In *Handbook of Functional Connectivity Magnetic Resonance Imaging Methods in CONN*, 17–25 (Hilbert, 2020).
31. Friston, K. J., Williams, S., Howard, R., Frackowiak, R. S. & Turner, R. Movement-related effects in fMRI time-series. *Magn. Reson. Med.* **35**, 346–355 (1996).
32. Hallquist, M. N., Hwang, K. & Luna, B. The nuisance of nuisance regression: spectral misspecification in a common approach to resting-state fMRI preprocessing reintroduces noise and obscures functional connectivity. *Neuroimage* **82**, 208–225 (2013).
33. Behzadi, Y., Restom, K., Liau, J. & Liu, T. T. A component based noise correction method (CompCor) for BOLD and perfusion based fMRI. *Neuroimage* **37**, 90–101 (2007).
34. Chai, X. J., Nieto-Castanon, A., Ongur, D. & Whitfield-Gabrieli, S. Anticorrelations in resting state networks without global signal regression. *Neuroimage* **59**, 1420–1428 (2012).
35. Nieto-Castanon, A. & Whitfield-Gabrieli, S. CONN functional connectivity toolbox: RRID SCR_009550, release 22. https://doi.org/10.56441/hilbertpress.2246.5840 (2022).
36. Desikan, R. S. et al. An automated labeling system for subdividing the human cerebral cortex on MRI scans into gyral based regions of interest. *Neuroimage* **31**, 968–980 (2006).
37. Nieto-Castanon, A. Functional connectivity measures. In *Handbook of Functional Connectivity Magnetic Resonance Imaging Methods in CONN*, 26–62 (Hilbert, 2020).
38. Nieto-Castanon, A. General Linear Model. In *Handbook of Functional Connectivity Magnetic Resonance Imaging Methods in CONN*, 63–82 (Hilbert, 2020).
39. Worsley, K. J. et al. A unified statistical approach for determining significant signals in images of cerebral activation. *Hum. Brain Mapp.* **4**, 58–73 (1996).
40. Nieto-Castanon, A. Cluster-level inferences. In *Handbook of Functional Connectivity Magnetic Resonance Imaging Methods in CONN*, 83–104 (Hilbert, 2020).
41. Chumbley, J., Worsley, K., Flandin, G. & Friston, K. Topological FDR for neuroimaging. *Neuroimage* **49**, 3057–3064 (2010).
42. van Maanen, L., Forstmann, B. U., Keuken, M. C., Wagenmakers, E. J. & Heathcote, A. The impact of MRI scanner environment on perceptual decision-making. *Behav. Res. Methods*. **48**, 184–200 (2016).
43. Kolodny, T. et al. Are attention and cognitive control altered by fMRI scanner environment? Evidence from Go/No-go tasks in ADHD. *Brain Imaging Behav.* **16**, 1003–1013 (2022).
44. Bush, G., Luu, P. & Posner, M. Cognitive and emotional influences in anterior cingulate cortex. *Trends Cogn. Sci.* **4**, 215–222 (2000).
45. Barkus, C. et al. Hippocampal NMDA receptors and anxiety: at the interface between cognition and emotion. *Eur. J. Pharmacol.* **626**, 49–56 (2010).
46. Stein, M. B., Simmons, A. N., Feinstein, J. S. & Paulus, M. P. Increased amygdala and insula activation during emotion processing in anxiety-prone subjects. *Am. J. Psychiatry* **164**, 318–327 (2007).
47. Hwang, K., Bertolero, M. A., Liu, W. B. & D'Esposito, M. The human thalamus is an Integrative Hub for functional brain networks. *J. Neurosci.* **37**, 5594–5607 (2016).

48. Paulus, M. P. & Stein, M. B. An insular view of anxiety. *Biol. Psychiatry* **60**, 383–387 (2006).
49. Etkin, A., Egner, T. & Kalisch, R. Emotional processing in anterior cingulate and medial prefrontal cortex. *Trends Cogn. Sci.* **15**, 85–93 (2011).
50. Harper, R. M. et al. Hypercapnic exposure in congenital Central Hypoventilation Syndrome reveals CNS respiratory control mechanisms. *J. Neurophysiol.* **93**, 1647–1658 (2005).
51. Kim, M. J. et al. Anxiety dissociates dorsal and ventral medial prefrontal cortex functional connectivity with the amygdala at rest. *Cereb. Cortex* **21 7**, 1667–1673 (2011).
52. Farhane-Medina, N. Z., Luque, B. & Tabernero, C. Castillo-Mayén, R. factors associated with gender and sex differences in anxiety prevalence and comorbidity: a systematic review. *Sci. Prog.* **105**, 00368504221135469 (2022).
53. Chaudhary, S. et al. Sex differences in the effects of trait anxiety and age on resting-state functional connectivities of the amygdala. *J. Affect. Disord. Rep.* **14**, 100646 (2023).

Acknowledgements

We sincerely thank the staff at DDRC Healthcare for their invaluable support in various aspects of this research, including gas filling and assistance with the setup.

Author contributions

DG – Contributed to the conception and design of the study, conducted the experiment, analyzed the data, and drafted the manuscript. SM – Contributed to the design of the experiment and assisted in conducting the experiment. GS – Reviewed the manuscript and facilitated the running of the experiment. AS – Reviewed the manuscript and provided critical revisions. JM – Reviewed the manuscript and provided critical revisions. SH – Contributed to the experimental design, data analysis, drafting and critical revision of the manuscript.

Funding

This work was supported by the University of Plymouth, School of Psychology, the Brain Research & Imaging Centre, and DDRC Healthcare as part of DG's PhD.

Declarations

Competing interests

The authors declare no competing interests.

Additional information

Correspondence and requests for materials should be addressed to D.G.

Reprints and permissions information is available at www.nature.com/reprints.

Publisher's note Springer Nature remains neutral with regard to jurisdictional claims in published maps and institutional affiliations.